Journal of Magnetic Resonance 209 (2011) 183–194

Contents lists available at ScienceDirect

Journal of Magnetic Resonance

journal homepage: www.elsevier.com/locate/jmr

Exact solution of the CPMG pulse sequence with phase variation down the echo train: Application to R_2 measurements

Alex D. Bain [a,*], Christopher Kumar Anand [b], Zhenghua Nie [c]

[a] Department of Chemistry and Chemical Biology, McMaster University, Canada
[b] Department of Computing and Software, McMaster University. Canada
[c] School of Computational Engineering and Science, McMaster University, Canada

ARTICLE INFO

Article history:
Received 22 November 2010
Available online 20 January 2011

Keywords:
CPMG experiments
Measurements of transverse relaxations
Rectangular pulses
Phase alternation
Phase cycling scheme
Bloch equations
Lagrange interpolation
Projection operators
Fitting models

ABSTRACT

An implicit exact algebraic solution of CPMG experiments is presented and applied to fit experiments. Approximate solutions are also employed to explore oscillations and effective decay rates of CPMG experiments. The simplest algebraic approximate solution has illustrated that measured intensities will oscillate in the conventional CPMG experiments and that using even echoes can suppress errors of measurements of R_2 due to the imperfection of high-power pulses. To deal with low-power pulses with finite width, we adapt the effective field to calculate oscillations. An optimization model with the effective field approximation and dimensionless variables is proposed to quantify oscillations of measured intensities of CPMG experiments of different phases of the π pulses. We show, as was known using other methods, that repeating one group of four pulses with different phases in CPMG experiments, which we call phase variation, but others call phase alternation or phase cycling, can significantly smooth the dependence of measured intensities on frequency offset in the range of $\pm\frac{1}{2}\gamma B_1$. In this paper, a second-order expression with respect to the ratio of frequency offset to π-pulse amplitude is developed to describe the effective R_2 of CPMG experiments when using a group phase variation scheme. Experiments demonstrate that (1) the exact calculation of CPMG experiments can remarkably eliminate systematic errors in measured R_2s due to the effects of frequency offset, even in the absence of phase variation; (2) CPMG experiments with group phase variation can substantially remove oscillations and effects of the field inhomogeneity; (3) the second-order expression of the effective decay rate with phase variation is able to provide reliable estimates of R_2 when offsets are roughly within $\pm\frac{1}{2}\gamma B_1$; and, most significantly, (4) the more sophisticated optimization model using an exact solution of the discretized CPMG experiment extends, to $\pm\gamma B_1$, the range of offsets for which reliable estimates of R_2 can be obtained when using the preferred phase variation scheme.

1. Introduction

Spin relaxation is widely applied to study molecular motion [1] such as chemical exchange [2,3], protein dynamics [4,5], and even the structure of invisible protein states which can be determined by applying relaxation dispersion [6,7]. Accurately measuring the relaxation rates, especially the transverse relaxation rates, is the key to fulfilling these studies. There are two ways to measure the transverse relaxation rates, one is using a single echo with a series of delay times [8], another one is to acquire the intensities after different numbers of echoes [9,10]. Although both of these two methods are going to suppress the B_0 field inhomogeneity, for several reasons, the second method is preferred.

The method which uses a single echo with a series of delays is called the Hahn echo [8]. It is a simple experiment and works well with a perfect pulse which can make the echo intensities to be a smooth exponential decay, but it lacks a mechanism to suppress oscillations of measured intensities which depend on the effects of imperfect pulses [9] or offsets [11]. However, there is an exact, and several approximate, solutions of the Hahn echo which provide some sophisticated analysis tools to account for oscillations due to pulse imperfections [11]. The second method for R_2 measurement, which uses a train of echoes, is called the CPMG pulse sequence [9,10]. Compared to Hahn echo experiments, CPMG experiments have several advantages. First, the frequency of the refocusing pulses provides information to study chemical exchange [3] and relaxation dispersion [7,12,13]. Second, the effects of J-coupling on measurements of R_2 will disappear if the delay time between the refocusing pulses of CPMG pulse sequences is sufficiently short [14], meaning that CPMG experiments may make the R_2 measurements of coupled spins more accurately than the

* Corresponding author. Address: Department of Chemistry and Chemical Biology, McMaster University, 1280 Main St. W., Hamilton, Ontario, Canada L8S 4M1. Fax: +1 905 522 2509.
E-mail address: bain@mcmaster.ca (A.D. Bain).

1090-7807/$ - see front matter © 2011 Elsevier Inc. All rights reserved.
doi:10.1016/j.jmr.2011.01.009

Hahn echo [15]. Third, the CPMG pulse sequence may suppress the effects of imperfect hard π pulses [9,10,16–18] and benefit by manipulating the inhomogeneous RF field of the surface coils [19]. More importantly, cycling the phases down the CPMG pulse train has been found to restrain the oscillations of measured intensities [12,13] with offset frequency. Instead of the conventional CPMG sequence of phases $\{x,x,x,x,\ldots,x\}$, Yip and Zuiderweg found that the sequence of phases $\{x,x,y,-y,x,x,y,-y,\ldots,x,x,y,-y\}$ gave significantly better performance [12]. We call this phase variation, but it could also be called phase cycling. Finally, the CPMG experiments can handle diffusion, whereas self-diffusion will limit longer transverse relaxations if using the Hahn echo to measure R_2 [9,10]. As a result, CPMG pulse sequences are widely applied to measure the transverse relaxation rates.

On the other hand, there are some challenges when applying CPMG experiments. CPMG experiments are more complicated than Hahn echo experiments. They will accumulate errors and these cumulative errors are not easily eliminated, neither when using hard pulses [20–29] nor soft pulses [30–33]. When applying hard pulses, CPMG experiments can suppress small errors due to imperfect pulses [9,10,20], but they still need to meet some conditions related to pulses, field inhomogeneity, stabilities in pulse timing and field-frequency ratio, and effects of diffusion if one is to obtain accurate R_2 estimates [20,22]. Outside these conditions, even using perfect hard pulses may result in unreliable measured R_2s when the offset of the pulse from resonance is bigger than about 10% of the amplitude of the π pulses [20].

Furthermore, soft pulses may exacerbate systematic errors in R_2 estimates [12,32]. As a consequence of limits of the probe and sample, it is necessary to perform CPMG experiments with soft π pulses and the delay time may be equal to the pulse width. Such wide pulses make the spin physics strongly dependent on offset frequency, because soft pulses induce rotation about tilted axes [12,32] and relaxation effects become significant [34]. Therefore, when applying soft pulses to do CPMG experiments, we have to be more careful in dealing with offsets and relaxation within pulses [12,32].

Processing CPMG data can be challenging [20,22,23,35], especially when soft π pulses are used [12,32]. Previously [11], we have found that an exact symbolic solution of the Hahn echo experiment incorporating offset and relaxation effects during pulses, delays and acquisition can be used to fit experimental data and obtain accurate R_2 estimates for a wider range of offsets than was previously possible. The goal of this paper is to similarly develop exact and approximate solutions of the Bloch equations for CPMG experiments (including soft π pulses) and, by fitting them to measurements, to obtain better R_2 estimates. In the first step, the general implicit exact solution of the CPMG experiments will be presented, then two approximations will be applied to explore the accuracy of CPMG experiments off resonance, and finally, we will fit our models to experimental data, validating the predicted wider range of frequencies for which accurate R_2 estimates can be obtained.

As we have seen, some strategies for good measurements of CPMG experiments such as using even echoes [9,10], making pulses close to resonance [20], and using specific phase variation schemes within the echo train [12] can improve the experiment. In this paper, we will quantify and explain these methods with the computation of CPMG experiments, and go beyond them. The simplest approximation confirms that using even echoes is better than using odd echoes in conventional CPMG experiments with high-power π pulses, and confirms the strong offset effect on the spin physics, and helps to elucidate the mechanism by which phase variation schemes suppress the oscillations present in low-power CPMG experiments. The computation introduces the second-order effective decay rate for the phase variation scheme of CPMG experiments, producing a smooth decay in the measured intensities.

2. Overview

In this paper, we restrict discussion to single-spin systems which can be described by the Bloch equations. The homogeneous form of the Bloch equations [36,37] is used:

$$\frac{d}{dt}\begin{pmatrix} M_x \\ M_y \\ M_z \\ M_e \end{pmatrix} = \begin{pmatrix} -1/T_2 & -\omega & \gamma B_1 \sin\phi & 0 \\ \omega & -1/T_2 & -\gamma B_1 \cos\phi & 0 \\ -\gamma B_1 \sin\phi & \gamma B_1 \cos\phi & -1/T_1 & 1/T_1 \\ 0 & 0 & 0 & 0 \end{pmatrix} \begin{pmatrix} M_x \\ M_y \\ M_z \\ M_e \end{pmatrix} \tag{1}$$

where ω is the resonance offset, γ is the gyromagnetic ratio, B_1 is the amplitude of the RF pulse, ϕ is the phase of the RF field with respect to the x axis, T_1 is the longitudinal relaxation time, T_2 is the transverse relaxation time and M_e is the equilibrium z magnetization which can be set as a constant number *1*. In the computation, the unit of offset and γB_1 is radians per second. In order to simplify the notations in the following sections, we define $b_1 \equiv \gamma B_1$, $R_1 \equiv \frac{1}{T_1}$, $R_2 \equiv \frac{1}{T_2}$, **A** to be the coefficient matrix and **M** the vector $(M_x, M_y, M_z, M_e)^T$, where T indicates transpose. If all parameters of the coefficient matrix are known, the simulation is easily carried out via numerical methods. The difficult task is to extract the unknown parameters we want, for example, T_2. We have solved the Hahn echo problem, and this is a continuation to deal with more complicated experiments using similar methods and notation of [11].

The Bloch equations have been solved in different ways [38–44]. Recently, we presented an elegant exact solution of the Bloch equations and applied it to the Hahn echo [11]. In this paper, we will continue to use the exact solution of the Bloch equations presented in [11]. Without loss of generality, the excitation pulse can be supposed to be perfect and it is along the y axis, thus, after the excitation pulse, the magnetization will be along with the x axis. We also use the numbers $\{0,1,2,3\}$ to represent the phases of pulses, corresponding to the x, y, $-x$ and $-y$ axes, respectively. A series of numbers, such as 0013, stands for a sequence of pulses with phases $\{x,x,y,-y\}$, following [12].

In the original Carr–Purcell experiments [9] using hard pulses, the major source of errors in R_2 is pulse imperfections. Meiboom and Gill then proposed that using even echoes with a shifted phase of excitation and π pulses would eliminate the error due to the imperfect amplitude of the hard π pulses [10]. We will explore this effect algebraically by expanding the even and odd intensities using a Taylor series in the offset frequency (ignoring relaxation effects).

If soft π pulses are used in CPMG experiments, offsets of the pulses from resonance significantly affect intensities. Conventional CPMG experiments fail to self-correct the errors even if the amplitude of the π pulses are perfectly adjusted [12,32]. When soft π pulses are applied to measure R_2, effects of offsets and R_1 contamination within π pulses cannot be ignored [11,12,32,34]. Different methods have been developed to eliminate these effects to improve the accuracy of measurements of R_2 including numerical correction, field gradients, adiabatic π pulses, and phase cycling [12,13,23,30–32,45,46]. Basically, these methods try to eliminate the errors due to offsets and then apply $T_{1\rho}$ as a major way to deal with the R_1 contamination within π pulses [12,13,32], meaning that CPMG experiments should meet the conditions of spin-lock $T_{1\rho}$ experiments [12]. However, we have known that the magnetization within a rectangular pulse is a combined decay, rather than a single decay [11,38], so we need a tool to deal with general CPMG experiments or provide more accurate approximations to analyze the measured intensities of special CPMG experiments, such as the phase cycling scheme presented in [12,13].

The Bloch equations of the homogeneous form within a pulse have four eigenvalues [11], one is zero, one is a real number which

corresponds to $T_{1\rho}$ [47], and other two are complex conjugates whose real part represents $T_{2\rho}$ [48] and imaginary part represents rotations around the effective rf field. All eigenvalues are independent of the phase of the pulse, but they depend on four parameters including the true R_1, R_2, the amplitude of the pulse and the offset (see Eqs. (10) and (11) of [11]). The phase of the pulse will decide the coefficients of these decay terms and rotation terms. So it is possible to choose a series of pulses with different phases which can make some coefficients of rotation terms as small as possible or only keep one decay term. Then we can suppress effects of the imperfect rotations due to offsets and obtain the effective R_2 [12,13].

The expression of the effective R_2 of one specific phase variation scheme has been provided in [12], but that expression does not include the effect of offset to the effective R_2. On the other hand, the eigenvalues of the Bloch equations show that the effective R_2 is not independent of offset. In this paper, a second-order expression of the effective R_2 including the effect of offset will be introduced. Experiments and simulations demonstrate the accuracy of this second-order approximation of the effective R_2 in a range of offsets a bit smaller than $\pm\frac{1}{2}\gamma B_1$.

Using the exact solution of the Bloch equations to extract R_2 via fitting was successful for Hahn echo experiments [11], but it is a challenge to find an explicit formula to calculate the CPMG experiments even when only considering the imperfect flip angles but not relaxation [20,49]. Because the CPMG experiments always repeat a pulse or a group of pulses, it can be calculated with a recursive method or the power of a matrix. It is straightforward to apply the recursive method with the exact solution of the Bloch equations to fit R_2. In this case, derivatives of the objective function can be computed using the chain rule [50]. The power of a matrix can be applied in the simplest approximations of CPMG experiments to qualitatively understand the source of oscillations or the effect of imperfections of hard π pulses.

3. Computation of CPMG experiments

CPMG experiments just repeat delays and echoes many times, thus, the intensity of CPMG experiments can be computed iteratively. A general implicit exact method to compute the CPMG experiments is presented, which can be applied to estimating the relaxation time or doing the simulation of CPMG experiments.

Because we have the exact solution of the Bloch equations [11] and all of the π pulses are identical in the conventional CPMG experiment [10], the exact solution of CPMG experiments can be computed by the iteration method (see Fig. 1),

$$\mathbf{M}_n = \mathbf{E}\mathbf{M}_{n-1} \tag{2}$$

where $\mathbf{M}_n$ and $\mathbf{M}_{n-1}$ respectively correspond to the magnetization vector after and before the nth echo, and

$$\mathbf{E} = \mathbf{E}_{\text{fid}}\mathbf{E}_{\pi}\mathbf{E}_{\text{fid}} \tag{3}$$

in which $\mathbf{E}_{\pi}$ is the exact solution of the Bloch equations of a π pulse and $\mathbf{E}_{\text{fid}}$ represents the effective matrix of a delay τ. So $\mathbf{E}$ is the exact solution of one echo. As explained previously, we can set, $\mathbf{M}_0 = (1,0,0,1)^T$, which is the state after a perfect excitation pulse along the y axis.

If we expand Eq. (2), the magnetization after the nth echo can be computed as

$$\mathbf{M}_n = \mathbf{E}^n\mathbf{M}_0 \tag{4}$$

In fact, $\mathbf{E}$ can also be applied to represent the solution of a combination of several pulses of different phases, for example, if we repeat one group of four pulses in CPMG experiments (Fig. 2), the effective matrix of the group of four pulses will be

$$\mathbf{E} = \mathbf{E}_{\text{fid}}\mathbf{E}_{\pi,\phi_4}\mathbf{E}_{\text{fid}}\mathbf{E}_{\text{fid}}\mathbf{E}_{\pi,\phi_3}\mathbf{E}_{\text{fid}}\mathbf{E}_{\text{fid}}\mathbf{E}_{\pi,\phi_2}\mathbf{E}_{\text{fid}}\mathbf{E}_{\text{fid}}\mathbf{E}_{\pi,\phi_1}\mathbf{E}_{\text{fid}} \tag{5}$$

The implicit solution of the CPMG experiments with phase (see Fig. 1) is calculated by

$$\mathbf{M}_n = \mathbf{E}_n\mathbf{M}_{n-1} \tag{6}$$

where

$$\mathbf{E}_n = \mathbf{E}_{\text{fid}}\mathbf{E}_{\pi}(\varphi_n)\mathbf{E}_{\text{fid}} \tag{7}$$

in which $\mathbf{E}_{\pi}(\varphi_n)$ is the exact solution of the nth π pulse with phase φ_n and $\mathbf{E}_n$ is the exact solution of the nth echo. Eq. (6) computes the magnetization at every echo, but we may only acquire the signal at the specific echoes, for example, every four echoes. Eq. (6) is also able to cope with non-equal delay spaces of CPMG experiments [51,52] or arbitrary pulse sequences if $\mathbf{E}_n$ represents the effective matrix of every step.

The eigen decomposition method has been applied to explore the solution of CPMG [20]. As we have known from the explicit solution of the Bloch equations, the explicit expression (usually derived by computer algebra) of $\mathbf{E}$ will be huge if intermediate variables are not used [11]. It will be a challenge to compute the eigenvalues and eigenvectors of the matrix $\mathbf{E}$ of entries with huge expressions. Thus, intermediate variables should be used in computing the full solution of the CPMG experiments, for example, we can define the matrix $\mathbf{E}$ with symbolic variables $E_{i,j}$ for the components of the solution for one echo Eq. (3), and then calculate the symbolic solution for eigenvalues and eigenvectors of the matrix $\mathbf{E}$ as a function of these variables. The Lagrange interpolation method has shown advantages to compute the exponential of a matrix [11], it also can be applied to compute the power of a matrix [53]. Basically, the full exact solution of CPMG experiments can be given by the Lagrange interpolation method with intermediate variables, whereas the explicit solution for CPMG experiments will be as unmanageable as the explicit solution of the Bloch equations [11].

Generally, the matrix $\mathbf{E}$ calculated by Eqs. (3) or (5) has four eigenvalues: one eigenvalue is *1*; one eigenvalue is a real number and the other two eigenvalues are complex conjugates [20], so the Lagrange interpolation method is applicable to the power compuation $\mathbf{E}^n$ [53,54]. The imaginary parts of these two conjugate eigenvalues result in oscillations of measured intensities in CPMG experiments. In order to get the symbolic expression, we need to reform the complex number into the polar form to compute the power of a complex number [55], this can be seen in the next section.

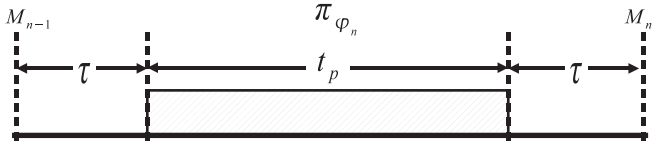

Fig. 1. The nth echo in CPMG experiments. Generally, in CPMG experiments, the amplitude and the length of the π pulses are fixed, but the phases of the π pulses may be different. τ is the delay time between the excitation pulse and the first π pulse, t_p is the length of the π pulse.

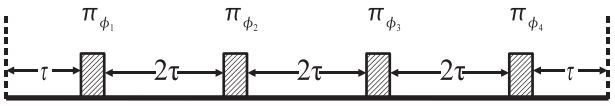

Fig. 2. One group of four pulses with different phases in CPMG experiments. We repeat this group to measure the intensities, which means that we do not acquire the intensities within this group. This group of phased pulses is the phase variation scheme $\phi_1\phi_2\phi_3\phi_4$.

4. Oscillations of conventional CPMG

Oscillations in Hahn echo intensities as a function of delay time are most sensitive to frequency offset [11]. In this section, we will explore the analogous effect on CPMG experiments along with the effect of echo number.

We use the simplest approximate model to compute the explicit solution of the basic CPMG experiment, without phase variation and ignoring the effects of relaxations, as an example of the method of computing the CPMG experiments presented in the previous section. This computation tells us that the oscillations of intensities will appear if the effective flip angle is not exactly π. It is possible to explicitly solve the simplest approximation of the CPMG cases with combinations of two-echo and four-echo pulses, but the results are not displayed in this paper.

Now consider the case that the effective flip angle is α which differs from π due to the pulse imperfections or offset effects ($\pi\sqrt{1+(\omega/\gamma B_1)^2}$). For example, the evolution associated with a π pulse with *0* phase between equal delays τ is **E**=

$$\begin{bmatrix} (1+\cos(\alpha))(\cos(\tau\omega))^2-\cos(\alpha) & -\sin(\tau\omega)\cos(\tau\omega)(1+\cos(\alpha)) & \sin(\alpha)\sin(\tau\omega) & 0 \\ \sin(\tau\omega)\cos(\tau\omega)(1+\cos(\alpha)) & -1+(1+\cos(\alpha))(\cos(\tau\omega))^2 & -\cos(\tau\omega)\sin(\alpha) & 0 \\ \sin(\alpha)\sin(\tau\omega) & \cos(\tau\omega)\sin(\alpha) & \cos(\alpha) & 0 \\ 0 & 0 & 0 & 1 \end{bmatrix} \tag{8}$$

The matrix **E** (Eq. (8)) can be diagonalized with the eigen decomposition method as

$$\mathbf{E}=\mathbf{PDP}^{-1} \tag{9}$$

where **D** is a diagonal matrix and the *i*th entry of **D** corresponds to the *i*th column vector of the eigenvector matrix **P**, then

$$\mathbf{E}^n=\mathbf{PD}^n\mathbf{P}^{-1} \tag{10}$$

It is easy to get the eigenvalues and eigenvectors of the matrix **E** (Eq. (8)) in Maple[1] and express the eigenvalues in the polar form of a complex number,

$$\boldsymbol{\lambda}=\begin{bmatrix} e^{i\phi_z} \\ e^{-i\phi_z} \\ 1 \\ 1 \end{bmatrix} \tag{11}$$

where

$$\phi_z=\arctan(y,x) \tag{12a}$$

$$y=\cos(\tau\omega)\sqrt{(1+\cos(\alpha))\left(2-(1+\cos(\alpha))(\cos(\tau\omega))^2\right)} \tag{12b}$$

$$x=-1+(\cos(\tau\omega))^2+\cos(\alpha)(\cos(\tau\omega))^2 \tag{12c}$$

ϕ_z is called the principal argument of a complex number defined as $0\leqslant\phi_z<2\pi$ [55]. Eigenvectors **P** and their inverse $\mathbf{P}^{-1}$ are not displayed.

Then, according to Eq. (4), the *z* magnetization after *n* echoes will be

$$M_{z,n}=\frac{\sin(\tau\omega)\sin(\alpha)(\cos(n\phi_z)-1)}{-2+(\cos(\tau\omega))^2+\cos(\alpha)(\cos(\tau\omega))^2} \tag{13}$$

[1] http://www.maple.com.

If relaxation is ignored, $\sqrt{M_x^2+M_y^2+M_z^2}$ will be equal to *1* at any time and the measured intensity after *n* echoes can be calculated as the following expression

$$s(n)\equiv\sqrt{M_{x,n}^2+M_{y,n}^2}=\sqrt{1-M_{z,n}^2} \tag{14}$$

Clearly, if $\sin(\tau\omega)\neq 0$ and $\sin\alpha\neq 0$, Eq. (13) tells us that the *z* magnetization may oscillate along with the number of the echoes unless $\phi_z=0$ which only occurs at isolated offsets (including on resonance), this means that the measured intensity of $\sqrt{M_x^2+M_y^2}$ will oscillate with different numbers of echoes when the π pulses are not perfect [20] or when soft π pulses are applied [12,32] in the conventional CPMG experiments [10].

Because α represents the flip angle, Eq. (14), which is simpler than the solution given in [49], is equivalent to the solution of CPMG of an imperfect hard π pulse when relaxations are ignored. In the following, we apply Eq. (14) to determine that using even-echo is better than using odd-echo in CPMG experiments of hard π pulses.

The simplified Taylor series of $s(n)$ evaluated at $\alpha=\pi$ is

$$s(n)\approx 1-1/8(\sin(\tau\omega))^2(\cos(n\pi)-1)^2(\alpha-\pi)^2+O((\alpha-\pi)^3) \tag{15}$$

where the big *O* notation represents the order of the error which can be seen as least-significant terms in the approximations.

So we get

$$s(2k+1)\approx 1-1/2(\sin(\tau\omega))^2(\alpha-\pi)^2+O((\alpha-\pi)^3) \tag{16}$$

$$s(2k)\approx 1+O((\alpha-\pi)^3) \tag{17}$$

where *k* is a non-negative integer. In fact, if we directly compute the Taylor series of Eq. (14) of an even number of echoes, we have

$$s(2k)\approx 1+O((\alpha-\pi)^6) \tag{18}$$

Evidently, $s(2k)$ will be more close to *1* and less sensitive to offset than $s(2k+1)$, which means that even-echo could suppress the error due to pulse imperfections [10]. We are able to apply the above method to investigate the performance of other combinations of even-echo pulses which are called phase alternation [16–18].

5. Applying optimization model on exploring oscillations

Eq. (13) only tells us that there may be oscillation in CPMG experiments, but we need more accurate models to predict its strength. Ignoring relaxation, the oscillation is zero when

$$f(n)=\sum_{k=1}^{n}\left(\sqrt{M_{x,k}^2+M_{y,k}^2}-\sqrt{M_{x,k-1}^2+M_{y,k-1}^2}\right)^2 \tag{19}$$

is zero. The larger the value of $f(n)$, the stronger the oscillation. Thus, we can formulate an optimization problem to find out the maximum value of $f(n)$ for a given range of offsets and delays with a given pulse sequence. If the maximum value of $f(n)$ is close to *0*, the measured intensities of using the given pulse sequence will not oscillate. In the following computation, we set $n=20$. By setting

Table 1
CPMG experiments with one identical pulse of a given phase. The table is obtained by solving the optimization problem for a given phase. For example, when the phase of the π pulse is along the x axis, the possible maximum difference between intensities along with the number of echoes will be 0.4 given at $\omega = \frac{1}{2}\gamma B_1$ and $\tau = 1.5t_p$ (see Fig. 3), this means that the difference of intensities of other offsets and delay times will be smaller than 0.4 for the given range of offsets and delays.

Phase	Maximum difference	$\omega/\gamma B_1$	τ/t_p
0	0.411	0.500	1.522
2	0.411	0.500	1.522
1	0.946	0.183	2.476
3	0.969	0.093	4.000

the index of M_k and M_{k-1} in Eq. (19) as $2k$ and $2(k-1)$ or $4k$ and $4(k-1)$, we are able to investigate CPMG experiments of applying the combinations of two or four pulses, if we compute the magnetization after every echo.

When the relaxations are ignored in CPMG experiments, the solution of one echo, $\mathbf{E}_n$, which is computed with the effective rotation field will be equivalent to the solution of Model 3 of [11] by setting $R_1 = 0$ and $R_2 = 0$ (see Appendix D.3 of [11]) and then $\mathbf{M}_k$ $(k = 1,\ldots,n)$ will be calculated by Eq. (6). In this analysis of the oscillation, two dimensionless variables are defined $\mu = \frac{\omega}{\gamma B_1}$ and $\delta = \frac{\tau}{t_p}$. A π pulse means that $\gamma B_1 t_p = \pi$. After applying these definitions in the optimization model which utilizes Eq. (6) as an equality constraint, variables would be $\mathbf{M}_k$ $(k = 1,\ldots,n)$, μ and δ. In [11], we determined that measuring R_2 using Hahn echo experiments is unreliable if the offset is larger than $\frac{1}{2}\gamma B_1$, so the bounds of the ratio of the offset and the amplitude of the pulse can be set as $0 \leqslant \mu \leqslant \frac{1}{2}$, this assumption matches the typical ^{15}N offsets of proteins on *600*MHz spectrometers when the amplitude of the π pulse is at least 2000 Hz [12,32]. Once the bounds of μ are decided, the upper bound of the ratio of the delay time over the pulse length δ can be set to *4* corresponding to an upper bound of $\omega\tau = 2\pi$. It is easy to code the optimization model in AMPL[2] [56] and solve the problem using IPOPT (Interior Point OPTimizer)[3] [57].

Tables 1–3 show the possible maximum systematic error in the intensities for given phases with respect to one pulse, groups of two pulses and groups of four pulses. The maximum difference of intensities corresponds to the maximum value of Eq. (19).

Because the objective functions are extremely non-linear and they have periodical terms such as trigonometric functions, the results shown in tables are only local optimal solutions with random initial variables of $\omega/\gamma B_1$ and τ/t_p, we have tried to resolve the optimization problems to get stable optimal solutions. The maximum difference of intensities tells us the strength of the oscillation. For example, if we measure the intensities at every echo, the intensities may oscillate within 40% if the phases are 0 or 2 (see Fig. 3), but if the phases are 1 or 3, the intensities of CPMG experiments may fluctuate between 0 and 1.

These three tables demonstrate that applying phase variation schemes can suppress oscillations in CPMG experiments. The scheme 0013 (originally observed in [12]) and schemes equivalent up to symmetry minimize the maximum oscillation to within 7% when $||\omega|| \leqslant \frac{1}{2}\gamma B_1$ and $\tau \leqslant 4t_p$. Fig. 4 illustrates that the magnetization is almost back to the x axis after one group of the phase variation scheme 0013. Thus, if relaxations are considered, the measured intensities of applying 0013 will decay smoothly for the given range of offset due to non-oscillations (see Fig. 10), and the sampling groups could be chosen arbitrarily. In the next section, we try to elucidate this good behaviour by considering the second-order approximation.

[2] http://www.ampl.com/.
[3] https://projects.coin-or.org/Ipopt; version: 3.8.1

Table 2
CPMG experiments with groups of two pulses. This table displays that the phase variation schemes 13 and 31 give the smallest oscillations among phase variation schemes with two pulses.

Phase	Maximum difference	$\omega/\gamma B_1$	τ/t_p
1–3	0.192	0.500	1.337
3–1	0.192	0.500	1.337
2–2	0.381	0.500	0.041
0–0	0.401	0.500	1.995
3–3	0.846	0.188	4.000
1–0	0.910	0.500	4.000
3–2	0.910	0.500	4.000
1–1	0.944	0.156	3.422
0–3	0.968	0.473	0.313
2–1	0.968	0.473	0.313
0–1	0.994	0.491	1.142
3–0	0.994	0.491	1.406
0–2	0.996	0.047	0.000
2–0	0.998	0.016	0.000
1–2	1.000	0.490	1.392
2–3	1.000	0.498	1.406

Table 3
CPMG experiments for the top eight phase variation schemes with four pulses. All other schemes have maximum differences greater than 0.10. Up to symmetries and similarities, all of these top eight phase variation schemes will be represented by one phase variation scheme 0013, as was independently derived in [12].

Phase	Maximum difference	$\omega/\gamma B_1$	τ/t_p
2–2–3–1	0.031	0.500	3.978
0–0–1–3	0.035	0.500	3.999
1–3–2–2	0.036	0.500	0.116
3–1–0–0	0.036	0.500	0.116
3–1–2–2	0.043	0.500	2.446
1–3–0–0	0.043	0.500	2.446
0–0–3–1	0.053	0.500	3.090
2–2–1–3	0.066	0.500	3.215

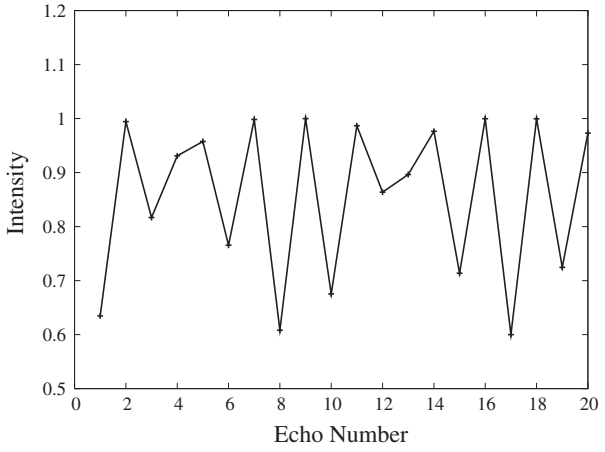

Fig. 3. Oscillations with respect to the echo number. This figure clearly displays that the measured intensities will oscillate between 1 and 0.6 along with the number of echoes when $\omega = \frac{1}{2}\gamma B_1$ and $\tau = 1.5t_p$. If there were no oscillations, all of intensities would be equal to 1.

6. Measured R_2 of CPMG experiments with phase cycle scheme of 0013

The previous section demonstrates that the 0013 phase variation scheme can suppress the oscillation of measured intensities of CPMG experiments when $||\omega|| \leqslant \frac{1}{2}\gamma B_1$. We see triangles of Fig. 10 which represents the measured intensities of applying the 0013 phase variation scheme decay smoothly and experiments of

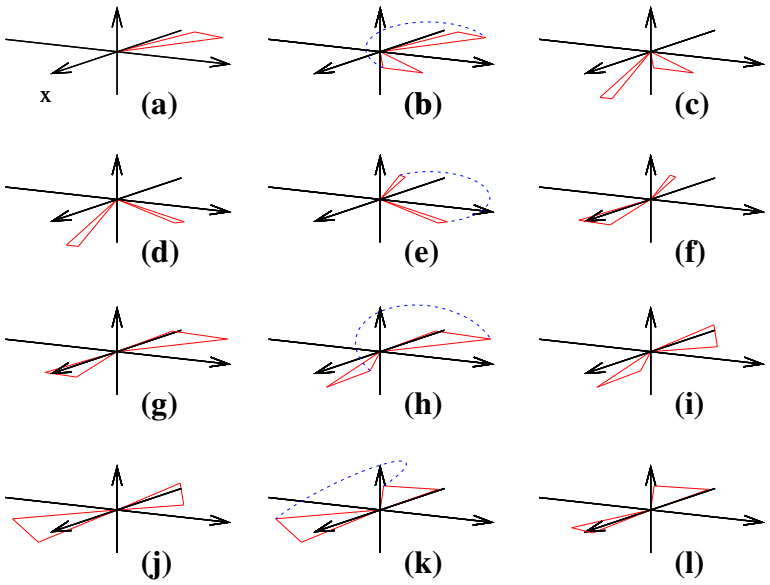

Fig. 4. Illustration of magnetization vectors of the phase variation scheme 0013. (b), (e), (h), and (k) display the effects of pulses. (a), (d), (g) and (j) show the magnetization before pulses (c), (f), (i) and (l) display the magnetizations after each echo. The initial magnetization is along the x axis, after one loop of 0013, the magnetization is almost parallel to the x axis again. (c) and (f) elucidate the advantage of even over odd echoes.

different offsets have different effective decay rates. The new question is what the effective decay rate of measured intensities is when the 0013 phase variation scheme is applied? Eq. (15) of [12] which is called the zeroth order expression (Eq. (26)) in our paper suggests that the effective R_2 is independent of offset, but Figs. 6 and 10 shows that the effective decay rates are not independent of offset, otherwise, the effective R_2s (green) of the *0013* phase variation scheme in Fig. 6 should be on a horizontal line with respect to the ratio of offset over pulse amplitude. The eigenvalues of the Bloch equations also tell us that the effective decay rates depend on offsets [11].

In this section, a second order approximation of effective decay rates with respect to the ratio of offset over the amplitude of the pulse evaluated on resonance will be obtained. The first step is to calculate the intensity on resonance of the 0013 phase variation scheme, then we will apply the effective rotation approximate solution of the Bloch equations which are called Model 3 in [11] to calculate the second order approximation of the intensities for offsets. Finally we will reproduce Fig. 6 of [12] with our new approximate formula and display the results of experiments.

[12] has shown that average magnetization of 0013 and 2231 must be implemented to measure R_2, thus in our computation and experiments, two scans are applied and the measured intensities will be computed by the average magnetization of applying these two phase variation schemes. So in the following, all intensities are computed as the average of two phase variation schemes, 0013 and 2231.

Using the exact solution of the Bloch equations, the explicit expression of the intensity of on-resonance of one loop of the phase variation scheme 0013 can be obtained. But normally, $R_1 \leqslant R_2 \ll \gamma B_1$, the second-order approximation of the eigenvalues of the Bloch equations of on-resonance with respect to the ratio of R_1/R_2 evaluated at $R_1/R_2 = 1$ is

$$\lambda = \begin{bmatrix} -R_2 \\ -1/2R_1 - 1/2R_2 + ib_1 \\ -1/2R_1 - 1/2R_2 - ib_1 \\ 0 \end{bmatrix} \tag{20}$$

where $i = \sqrt{-1}$. The general solution of the Bloch equations of on-resonance can be obtained by substituting λ of Eq. (13) of [11] with Eq. (20). Considering the phases and t_p b1 = π, we have effective matrices $\mathbf{E}_{\pi,0}$, $\mathbf{E}_{\pi,1}$, $\mathbf{E}_{\pi,2}$, $\mathbf{E}_{\pi,3}$ of π pulses corresponding to phases $x, y, -x, -y$, then we obtain the effective matrices of 0013 and 2231,

$$\mathbf{E}_{0013} = \mathbf{E}_{\text{fid}}\mathbf{E}_{\pi,3}\mathbf{E}_{\text{fid}}\mathbf{E}_{\text{fid}}\mathbf{E}_{\pi,1}\mathbf{E}_{\text{fid}}\mathbf{E}_{\text{fid}}\mathbf{E}_{\pi,0}\mathbf{E}_{\text{fid}}\mathbf{E}_{\text{fid}}\mathbf{E}_{\pi,0}\mathbf{E}_{\text{fid}} \tag{21}$$

$$\mathbf{E}_{2231} = \mathbf{E}_{\text{fid}}\mathbf{E}_{\pi,1}\mathbf{E}_{\text{fid}}\mathbf{E}_{\text{fid}}\mathbf{E}_{\pi,3}\mathbf{E}_{\text{fid}}\mathbf{E}_{\text{fid}}\mathbf{E}_{\pi,2}\mathbf{E}_{\text{fid}}\mathbf{E}_{\text{fid}}\mathbf{E}_{\pi,2}\mathbf{E}_{\text{fid}} \tag{22}$$

and the average magnetization of two phase variation schemes,

$$\mathbf{M}_4 = \frac{1}{2}(\mathbf{E}_{0013} + \mathbf{E}_{2231})\mathbf{M}_0 \tag{23}$$

because $\mathbf{M}_4[2]$ which is the magnetization along the y axis is *0*, the on-resonance intensity of one loop which is the magnetization along the x axis, $\mathbf{M}_4[1]$, is

$$\begin{aligned}
&\left(\frac{(R_1-R_2)^4}{\left((R_1-R_2)^2+4b_1^2\right)^2}\left(e^{-2(\tau+t_p)R_2}+\frac{b_1^2e^{-2R_2t_p-2\tau R_1}}{R_2^2}\right)\right.\\
&+\frac{16(R_1-R_2)^4R_1^2b_1^2e^{-(2\tau+t_p)R_1-R_2t_p}}{\left((R_1-R_2)^2+4b_1^2\right)\left((R_1+R_2)^2+4b_1^2\right)\left(\left(R_1^2-R_2^2\right)^2+8b_1^2\left(R_1^2+R_2^2+2b_1^2\right)\right)}\\
&+\frac{8(R_1-R_2)^4R_1b_1^2e^{-3/2R_2t_p-(2\tau+1/2t_p)R_1}}{R_2\left((R_1-R_2)^2+4b_1^2\right)\left(\left(R_1^2-R_2^2\right)^2+8b_1^2\left(R_1^2+R_2^2+2b_1^2\right)\right)}\\
&+\frac{-8(R_1-R_2)^2b_1^2e^{-1/2t_pR_1-(2\tau+3/2t_p)R_2}}{\left((R_1-R_2)^2+4b_1^2\right)^2}\\
&\left.+\frac{16b_1^4e^{-t_pR_1-(2\tau+t_p)R_2}}{\left((R_1-R_2)^2+4b_1^2\right)^2}\right)e^{-2R_2(t_p+3\tau)}
\end{aligned} \tag{24}$$

We are able to further simplify by ignoring low-order terms (in terms of the pulse amplitude), resulting in the approximation of the intensity on resonance of applying one loop of the phase variation scheme 0013:

$$e^{-8\tau R_2 - t_pR_1 - 3R_2t_p} \tag{25}$$

Therefore, the effective R_2 on resonance when applying the 0013 phase variation scheme will be

$$R_{2-eff}^{0013^{\text{on-resonance}}} = R_2 + \frac{(R_1-R_2)t_p}{8\tau + 4t_p} \tag{26}$$

which is the same as Eq. (15) of [12]. As we said before, we focus on $||\omega|| \leqslant \frac{1}{2}\gamma B_1$ in this paper, which means that Eq. (26) is the zeroth order approximation of the effective R_2 with respect to the ratio $\omega/\gamma B_1$ evaluated on resonance, the computation shows that Eq. (26) is also the first order approximation of the effective R_2 with respect to the ratio of $\omega/\gamma B_1$. Eq. (26) is not suitable for describing the behaviour of large offsets outside of $-15\% \sim 15\%$ of γB_1 [12,13]. In the following, we will deduce the second order approximation of the effective relaxation rate with respect to $\omega/\gamma B_1$.

We are able to calculate the intensity with offsets by using the second-order approximation of the eigenvalues (see Eq. (18) of [11]) as we did for on resonance intensity, but the expression is not simple enough to identify these significant terms. In order to simplify our computation, a soft π pulse is approximated by an effective rotation field of $t_p\sqrt{\omega^2 + b1^2}$ with two on-resonance delays of $t_p/2$ (see Fig. 5), which is one of the second-order split methods called Model 3 in our previous work [11] to compute the approximate solution of the Bloch equations displayed in [11]. The solution of Model 3 is displayed in Appendix D.3 of [11]. Substituting $\mathbf{E}_{\pi,0}$, $\mathbf{E}_{\pi,1}$, $\mathbf{E}_{\pi,2}$, $\mathbf{E}_{\pi,3}$ of Eqs. (21) and (22) with the approximate solution of the Bloch equations with offsets, we calculate the magnetization vector Eq. (23). Then the intensity is $\sqrt{M_4[1]^2 + M_4[2]^2}$. Setting $\mu = \omega/b1$, the second-order approximation of the measured intensity of one loop of 0013 with respect to μ evaluated at $\mu = 0$ is

$$e^{-4R2(2\tau+t_p)}\left(1 + 4(e^{-(2\tau+t_p)(R1-R2)} - 1)\mu^2\right) + O(\mu^3) \tag{27}$$

Because two different approximate methods are used to calculate Eqs. (25) and (27), we see that the constant term of Eq. (27) is not the the same as Eq. (25). Model 3 approximates the effective decay as R_2, which does not include the R_1 contamination even on resonance. So Eq. (25) will be more accurate to represent the measured intensity on resonance of one loop of 0013 than $e^{-4R2(2\tau+t_p)}$. Based on the discussion, we if substitute $e^{-4R2(2\tau+t_p)}$ of Eq. (27) with Eq. (25), then we obtain the second-order approximation of the measured intensity of one loop of the phase variation scheme 0013 with respect to μ evaluated at $\mu = 0$ is

$$e^{-8\tau R_2 - t_p R_1 - 3R_2 t_p}\left(1 + 4(e^{-(2\tau+t_p)(R1-R2)} - 1)\mu^2\right) + O(\mu^3) \tag{28}$$

Thus, the second-order effective R_2 will be

$$R_{2-eff}^{0013} = R_2 + \frac{(R_1 - R_2)t_p}{8\tau + 4t_p} + \frac{1 - e^{-(2\tau+t_p)(R1-R2)}}{2\tau + t_p}\mu^2 + O(\mu^4) \tag{29}$$

If the delay time is chosen to make

$$-(2\tau + t_p)(R_1 - R_2) \ll 1 \tag{30}$$

Eq. (29) can be simplified as

$$R_{2-eff}^{0013} = R_2 + \frac{(R_1 - R_2)t_p}{8\tau + 4t_p} + (R_1 - R_2)\mu^2 \tag{31}$$

If we substitute offset and pulse amplitude back into Eq. (31), consider that $t_p b_1 = \pi$ and change the unit of offset to Hertz, we have

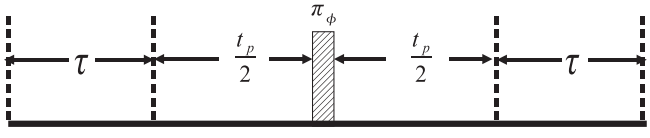

Fig. 5. Approximation of one echo which is called Model 3 in [11]. The hatched rectangle represents effective rotations. A soft π pulse is approximated by an effective rotation of $t_p\sqrt{\omega^2 + b1^2}$ with two on-resonance delays of $t_p/2$. Although this approximation provides a good performance [11], R_1 contamination cannot be observed in this approximation because the relaxations within the pulse are split out.

$$R_{2-eff}^{0013} = R_2 + \frac{(R_1 - R_2)t_p}{8\tau + 4t_p} + (R_1 - R_2)(2t_p v)^2 \tag{32}$$

where v represents the offset in Hz.

Supposing we obtain the effective R_2 of 0013 experiments by fitting e^{-tR2}, then the following formula will give the true R_2 based on Eq. (29),

$$R_2 = R_{2-eff} - \frac{t_p(R1 - R_{2-eff})}{8\tau + 3t_p} - \frac{4\left(1 - e^{\frac{-4(2\tau+t_p)^2(R1-R_{2-eff})}{8\tau+3t_p}}\right)}{8\tau + 3t_p}\mu^2 + O(\mu^4) \tag{33}$$

Eq. (33) could also be simplified under the condition Eq. (30).

We can do 0013 CPMG experiments, and fit the data to $e^{-t\ R2}$ to obtain the effective R_2 directly in Bruker's TOPSPIN, and then apply Eq. (33) to estimate the true R_2. Results of simulation and experiments illustrate this methodology.

Fig. 6 reproduces the simulation in Fig. 6 of [12] as well as the second-order expression of the effective decay rate, Eq. (29). In this

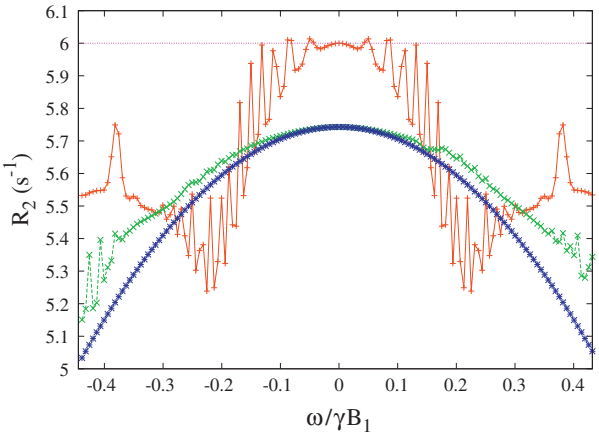

Fig. 6. Simulated profile of effective decay rates of CPMG experiments of soft π pulses. Reproduced Fig. 6 of [12], with offset/pulse amplitude on the horizontal axis, and R_2 (s^{-1}) on the vertical. Parameters are the same as [12]. $\tau = 250$ μs, $t_p = 200$ μs, $R_1 = 2.4\ s^{-1}$, true $R_2 = 6\ s^{-1}$, $\gamma B_1 = 2500$ Hz. The sampling points are at loops: 2, 12, 35. The red curve represents 0000, the green curve 0013, the blue curve plots Eq. (29) with the same parameters. (For interpretation of the references to colour in this figure legend, the reader is referred to the web version of this article.)

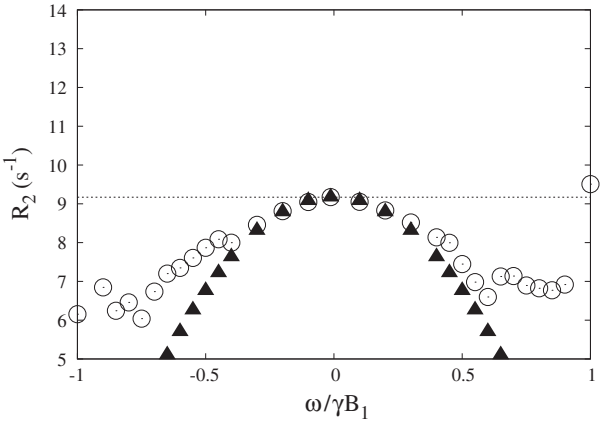

Fig. 7. The profile of measured effective R_2 using 0013 phase variation with respect to offsets. The circles represent the measured R_2 fitted by the function e^{-tR_2}, the triangle points are given by Eq. (29). Most of these points within $\pm\frac{1}{2}\gamma B_1$ match well. The parameters and descriptions of the experiments are displayed in the next section.

simulation, the excitation pulse is along the y axis, the intensities are computed at loops 2, 12, and 35 with the average magnetization from phase variation schemes 0000 and 2222, or 0013 and 2231, respectively. Fitting these intensities with e^{-tR_2}, we get the effective measurements of R_2 (red and green curves of Fig. 6). The blue curve of Fig. 6 is plotted using Eq. (29). If we change the sampling loops or increase the sampling numbers, the red curve may be different because of oscillations, but the green curve may not change, especially when offsets are smaller. This implies that the sampling loops of the *0013* phase variation scheme can be choosen arbitrarily.

Fig. 7 is obtained from CPMG experiments using the 0013 phase variation scheme which are described in the next section. Both Figs. 6 and 7 confirm that Eq. (29) predicts the effective R_2 accurately approximately within $\pm\frac{1}{2}\gamma B_1$ which is much wider than the range of $\pm 0.15\gamma B_1$ given by Eq. (26) in [12] and the range investigated in [13].

As the 0013 phase variation scheme can eliminate the intensity oscillations and spins mostly refocus after one loop, the effects of the B_0 and B_1 inhomogeneity may be restrained as well. Eq. (29) demonstrates that 1% error of the ratio of offset over the amplitude

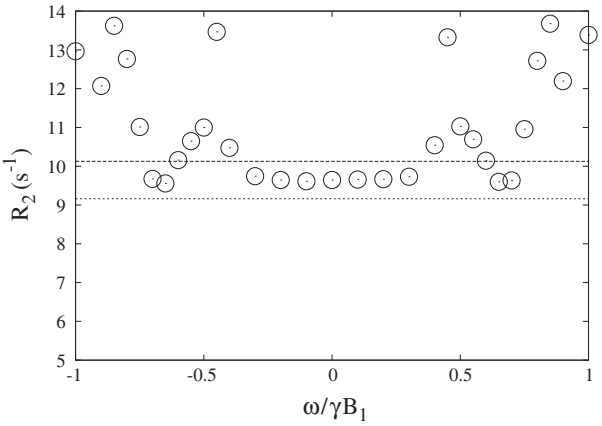

Fig. 9. The profile of measured R_2 from conventional CPMG experiments plotted with respect to ratio of offset over the amplitude of the π pulse. The two dotted lines correspond to ±5% of 9.64 s^{-1} which is the measured on-resonance R_2. This figure shows that offset effects can be eliminated by fitting the exact solution of the Bloch equations, when $\|\omega\| \leqslant 0.3\gamma B_1$ which is narrower than the range of $0.5\gamma B_1$ we observed in [11], possibly because CPMG experiments accumulate the inhomogeneity effects.

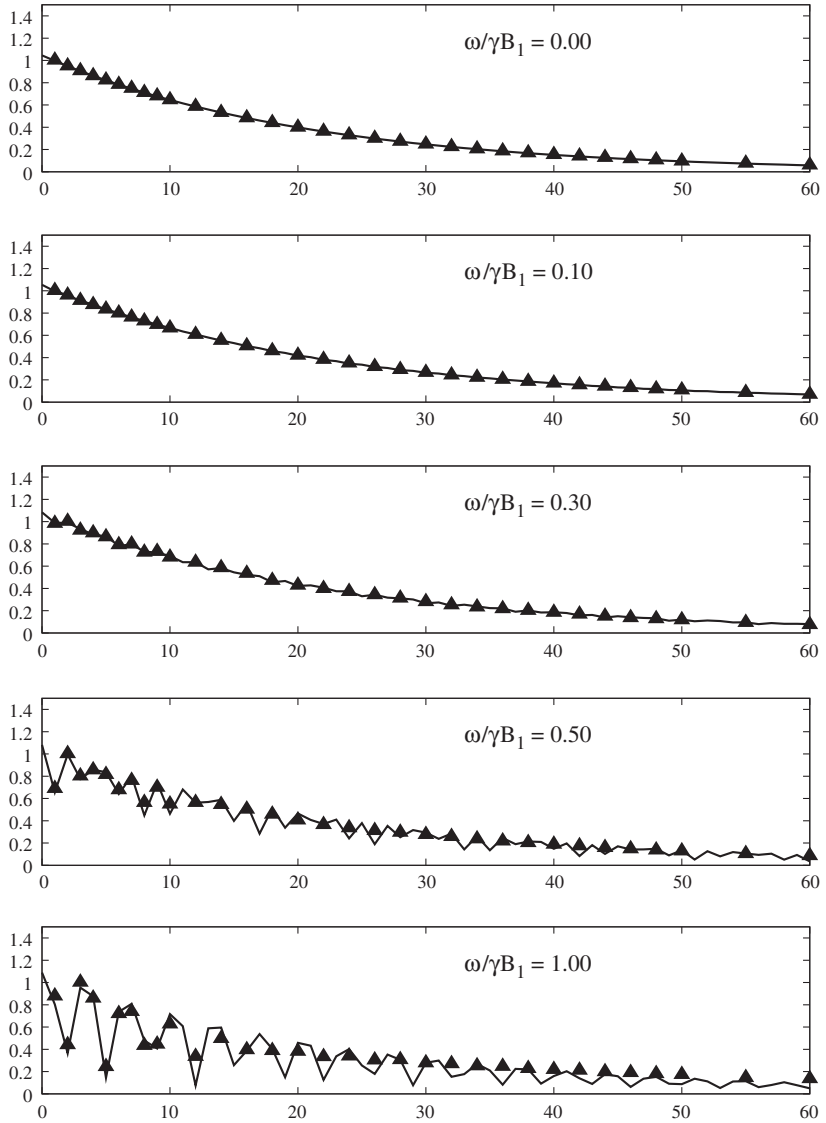

Fig. 8. Fitted curves and measured intensities of the conventional CPMG experiments. The x axis is the echo number, the y axis is the intensity, normalized so that the maximum measured intensity is *1*. The triangles are measured intensities, the curves are the results of fitting the exact solution of the Bloch equations. The offsets are 0.0, 50, 150, 250, and 500 Hz corresponding to the ratio of $\frac{\omega}{\gamma B_1}$ $\{0, 0.10, 0.30, 0.50, 1.00\}$ from the top to the bottom, the measured R_2 are 9.64, 9.66, 9.73, 11.03, and 13.39 s^{-1}, respectively. In all cases, $R_1 = 0.227$ s^{-1}.

of the pulse only result in 2% error of the second-order terms of effective R_2. Numerical simulations also verify that variations of offset or the pulse amplitude have less effects of measurements of R_2 using the 0013 phase variation scheme than using the conventional CPMG experiments when the offsets are within half of the pulse amplitude.

7. Fitting CPMG experiments with the exact solution

In [11], we found that by using the exact solution of the Bloch equation for data fitting, we could eliminate offset effects for Hahn echo data when $||\omega|| \leqslant \frac{1}{2}\gamma B_1$. In this section, we will similarly show how to estimate R_2 from CPMG data using the exact solution of the Bloch equations and compare the measurements of R_2 using the 0013 phase variation scheme given by Eq. (33).

Eq. (6) is the formula to compute the magnetization after the nth echo, which we fit to the measured intensities in CPMG experiments using the objective

$$\min \sum_{k=1}^{K} \left\| M_{meas}[k] - I_0 \sqrt{M_{x,m[k]}^2 + M_{y,m[k]}^2} \right\|^2 \tag{34}$$

where $M_{meas}[k]$ is the kth measured intensity, and $M_{x,y,m[k]}$ computed by Eq. (6) are magnetizations at the $m[k]$th echo which correspond to the kth measured intensity. Supposing that the array of m which stores the index of echo numbers corresponding to the kth measured intensity is in the ascending order, the maximum echo number will be $m[K]$ which is the size of the arrays of M_x, M_y and M_z, where K is the number of measured points. If considering multiple scans, the arrays can be set as two-dimensional arrays, one dimension will represent the scan number.

The experiments were performed on Bruker AVANCE 500 MHz spectrometer with the Shigemi tube and a 5 mm inverse geometry probe, the sample was cyclohexane and the solvent was $CDCl_3$, the temperature was adjusted to 280 K, the amplitude of the π pulse was equivalent to 500 Hz which means that the length of the π pulses was 0.001 s. The excitation pulse was along the y axis and the length of the excitation pulse (equivalent to 30,300 Hz) was

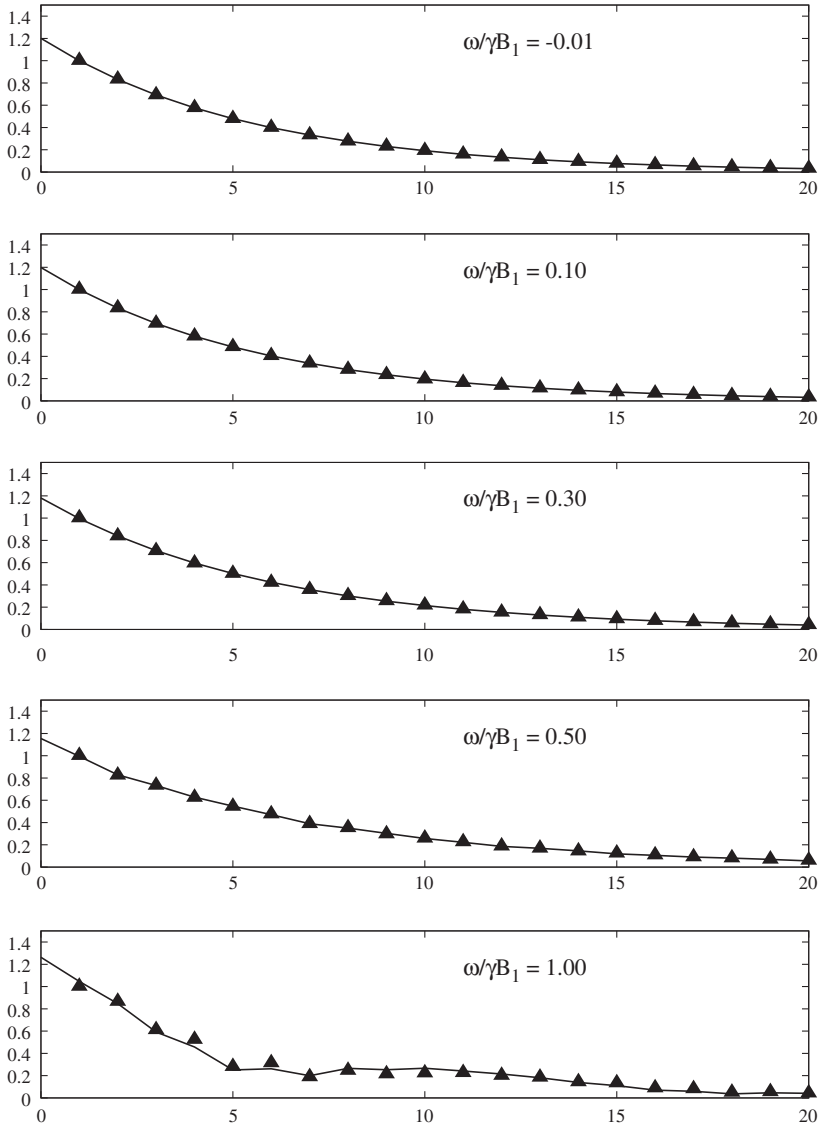

Fig. 10. Fitted curves and measured intensities for phase variation scheme 0013. Normalized intensity is plotted against echo number divided by four. The triangles are measured intensities, the curves are the result of fitting the exact solution of the Bloch equations. The offsets are −6.28, 50, 150,250, and 500 Hz corresponding to $\frac{\omega}{\gamma B_1}$ ratios of $\{-0.01, 0.10, 0.30, 0.50, 1.00\}$. The effective R_2s are 9.17, 9.05, 8.52, 7.44 and 9.50 s^{-1} and the measured true R_2s are 9.65, 9.59, 9.55, 9.69 and 10.82 s^{-1}, respectively. In all cases, $R_1 = 0.227\ s^{-1}$.

8.25 μs. The delay time between the excitation pulse and the first π pulse was set to 0.002 s. The pre-scan delay called *DE* in Bruker spectrometers was 6.5 μs. The measured R_1 was 0.227 s^{-1} and the measured R_2 obtained by the conventional CPMG experiment with high-power pulses on resonance was 9.84 s^{-1}.

Two sets of experiments with a range of offsets and two different phase-variation strategies were performed: the conventional CPMG experiments with phases $\pm x$, and modified CPMG with phases $\{\pm x, \pm x, \pm y, \mp y\}$, i.e. 0013 and 2231. The phase of the receiver coil was set to 0. The data for each experiment was collected with two scans (one scan is the 0013 phase variation scheme and another is 2231. These two scans can also be performed with excitation pulse alternation of one phase variation scheme [12]), and the measured intensities were obtained using TOPSPIN software. The measured R_2 obtained by the conventional CPMG experiment using soft pulses on resonance was 9.64 s^{-1} and the measured R_2 obtained by the 0013 CPMG experiment using soft pulses at −6.28 Hz was 9.65 s^{-1}. The error of these measurements of R_2 is 2% relative to the measured R_2 obtained by the CPMG experiment with high-power pulses.

The optimization model matching the pulse programs was coded to the C++ interface of IPOPT [57] using the exact gradient and Hessian of the objective function. The C++ code of the exact solution of the Bloch equations and its first-order and second-order partial derivatives with respect to R_2 was generated by the *codegen* function in Maple, the chain rule [50] was applied to take advantage of the intermediate variables to efficiently compute the gradient and Hessian of the objective function. With exact second-order derivatives, the underlying methods used by IPOPT converge quadratically (versus linearly with only first-order derivatives) and are more robust [57]. All solver options were used the default value except the iteration number of *500* and the initial values of $I_0 = 1$ and $R_2 = 9.84$.

In order to simplify the computation, the magnetization after a hard excitation pulse can be set as $(1,0,0,1)^T$, but if the excitation pulse is not a hard pulse, the fitting model should include effects of the excitation pulse. The fitting model can also incorparate the effects of B_0 and B_1 inhomogeneity as explained in [11]. In this paper, the fitting model does not incorporate the field inhomogeneity, but the model does incorporate the effects of the excitation pulse.

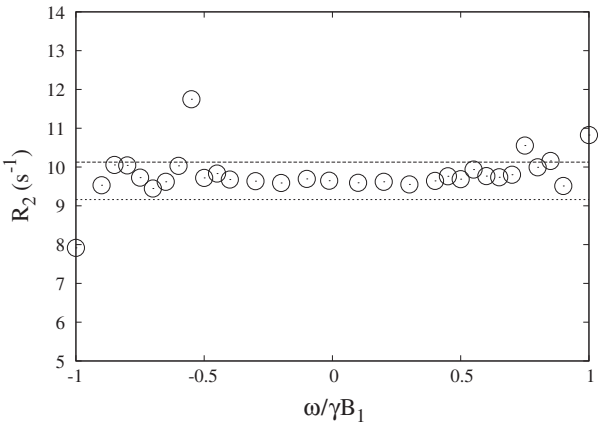

Fig. 11. Measured R_2 of the phase variation scheme 0013 plotted against the ratio of offset over the amplitude of the π pulse. The two dotted lines represent ±5% of 9.64 s^{-1}, R_2 measured on resonance. Fitting the exact solution to 0013 data effectively eliminates the effects on measured R_2 of offsets within the amplitude of the π pulse except some values, which is significantly wider than the conventional CPMG experiments shown in Fig. 9. This figure also validates that the 0013 phase variation scheme can suppress the effects of the inhomogeneity. We see there is one exception at $\omega/\gamma B_1 = -0.55$ corresponding to −275 Hz.

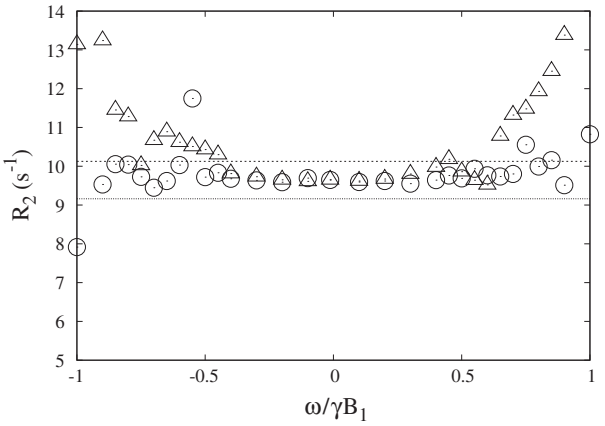

Fig. 12. Measured R_2 of the phase variation scheme 0013 plotted against the ratio of offset over the amplitude of the π pulse, including circles for exact solution fitting from Fig. 11 and triangles obtained by fitting Eq. (33) to the same experiment data (the circle points in Fig. 7). This figure tells us that fitting the exact solution of the Bloch equations provides allows us to cover almost twice the offset frequency range in one experiment.

Fig. 8 makes apparent the oscillation in measured intensities in conventional CPMG experiments. Although both of Fig. 9 and Fig. 8 of [11] were fitted by the exact solution of the Bloch equations, the offset range of the conventional CPMG experiments, which can provide reliable measurements of R_2, is narrower than the range using the Hahn echo experiments. This comparison illustrates that conventional CPMG experiments accumulate errors due to field inhomogeneity.

Fig. 10 exhibits the reduced oscillations in measured intensities associated with the 0013 phase variation scheme. Fig. 11 reveals that it is possible to acquire reliable R_2 estimates when offsets are roughly within γB_1.

Figs. 9 and 11 demonstrate that the fitting procedures using the exact solution of the Bloch equations can provide reliable measurements of R_2 in a wide range. Moreover, the 0013 phase variation scheme can cover a much wider range than the conventional CPMG experiments, showing that the phase variation scheme 0013 can suppress the effects of the B_0 and B_1 inhomogeneity.

Fig. 12 confirms that the second-order effective R_2 expression (Eq. (29)) or the second-order corrections of measurements of R_2 (Eq. (33)) are reliable to analyze CPMG experiments of the 0013 phase variation scheme in a specific offset range, considerably smaller than obtained by fitting to the exact solution. If the reduced range is sufficient, however, fitting to the second-order approximation is easier to implement.

8. Conclusion

In this paper, we used exact and approximate solutions of the Bloch equations for CPMG experiments to investigate the performance of these experiments. We explored the oscillations of conventional CPMG experiments and applied Taylor series to show that using even echoes of hard pulses, we can reduce the error due to pulse imperfections. We also proposed a method of investigating oscillations in measured intensities at different echoes, the effect of different phases of π pulses and the minimization of those oscillations with respect to the phase variation scheme. Soft π pulses make the data processing more complicated because relaxation and offset cannot be ignored within pulses. A second-order expression of the effective R_2 under the 0013 phase variation scheme was deduced from the solutions of the Bloch equations. Simulations and experiments indicate that this second-order

approximation is valid when offsets are roughly within $\pm\frac{1}{2}\gamma B_1$ of resonance. The exact solution of the Bloch equations was also applied to fit CPMG data. The experiments revealed that the 0013 phase variation scheme can not only provide non-oscillated measured intensities, but also suppress the effects of the field inhomogeneity. Without considering inhomogeneity, but using the exact solution of the Bloch equations, the 0013 scheme can deliver reliable R_2 measurements when offsets are almost everywhere within $\pm\gamma B_1$ which is much wider than the accurate offset range for the conventional CPMG experiments. The accurate offset range for the conventional CPMG experiment is even smaller than the second-order method or the Hahn echo experiments [11]. We saw that if offsets are roughly within $\pm\frac{1}{2}\gamma B_1$, the fitting to the second-order expression of the effective R_2 is as good as fitting to the exact solution. If, however, the absolute values of offsets are between $\frac{1}{2}\gamma B_1$ to γB_1, the exact solution of the Bloch equations should be applied to extract accurate R_2s. If the offsets are not within $\pm\gamma B_1$, measured R_2 may be unreliable. Without doubt, the fitting to the exact solution provides a worthwhile improvement, meaning that it is important to develop data-processing methods. As we have seen in this paper and [11], even when we use the exact solution of the Bloch equations, field inhomogeneity will rob the process of accuracy outside some offset range. If the distribution of the inhomogeneity can be fully mapped, it is possible to improve the fitting results [11], but it is a challenge to exactly map the inhomogeneity [58]. In the future, we hope to design optimal shaped universal rotation pulses which can overcome the B_1 inhomogeneity and provide uniform spectroscopy of CPMG experiments in an even wider range of offsets and then we will apply these optimal pulses to measure R_2.

Acknowledgment

Alex D. Bain and Christopher Anand would like to thank the Natural Science and Engineering Research Council of Canada (NSERC) for financial support.

References

[1] M.H. Levitt, Spin Dynamics: Basics of Nuclear Magnetic Resonance, John Wiley & Sons, Chichester, New York, 2001.
[2] A. Allerhand, E. Thiele, Analysis of Carr–Purcell spin-echo NMR experiments on multiple-spin systems. II. The effect of chemical exchange, J. Chem. Phys. 45 (1966) 902–916.
[3] A.D. Bain, Chemical exchange in NMR, Prog. Nucl. Magn. Reson. Spectrosc. 43 (2003) 63–103.
[4] M.W.F. Fischer, A. Majumdar, E.R.P. Zuiderweg, Protein NMR relaxation: theory, applications and outlook, Prog. Nucl. Magn. Reson. Spectrosc. 33 (1998) 207–272.
[5] D.D. Boehr, H.J. Dyson, P.E. Wright, An NMR perspective on enzyme dynamics, Chem. Rev. 106 (2006) 3055–3079.
[6] D.F. Hansen, P. Vallurupalli, L.E. Kay, Using relaxation dispersion NMR spectroscopy to determine structures of excited, invisible protein states, J. Biomol. NMR 41 (2008) 113–120.
[7] P. Vallurupalli, D.F. Hansen, P. Lundström, L.E. Kay, CPMG relaxation dispersion NMR experiments measuring glycine $^1H^\alpha$ and $^{13}C^\alpha$ chemical shifts in the 'invisible' excited states of proteins, J. Biomol. NMR 45 (2009) 45–55.
[8] E.L. Hahn, Spin echoes, Phys. Rev. 80 (1950) 580–594.
[9] H.Y. Carr, E.M. Purcell, Effects of diffusion on free precession in nuclear magnetic resonance experiments, Phys. Rev. 94 (1954) 630–638.
[10] S. Meiboom, D. Gill, Modified spin-echo method for measuring nuclear relaxation times, Rev. Sci. Instrum. 29 (1958) 688–691.
[11] A.D. Bain, C.K. Anand, Z. Nie, Exact solution to the bloch equations and application to the Hahn echo, J. Magn. Reson. 206 (2010) 227–240.
[12] G.N.B. Yip, E.R.P. Zuiderweg, A phase cycle scheme that significantly suppresses offset-dependent artifacts in the R_2-CPMG ^{15}N relaxation experiment, J. Magn. Reson. 171 (2004) 25–36.
[13] D. Long, M. Liu, D. Yang, Accurately probing slow motions on millisecond timescales with a robust NMR relaxation experiment, J. Am. Chem. Soc. 130 (2008) 2432–2433.
[14] L.A. Stables, R.P. Kennan, A.W. Anderson, J.C. Gore, Density matrix simulations of the effects of J coupling in spin echo and fast spin echo imaging, J. Magn. Reson. 140 (1999) 305–314.
[15] S.R. Williams, D.G. Gadian, E. Proctor, D.B. Sprague, D.F. Talbot, I.R. Young, F.F. Brown, Proton NMR studies of muscle metabolites *in Vivo*, J. Magn. Reson. 63 (1985) 406–412.
[16] A.A. Maudsley, Modified Carr–Purcell–Meiboom–Gill sequence for NMR Fourier imaging applications, J. Magn. Reson. 69 (1986) 488–491.
[17] A.J. Shaka, S.P. Rucker, A. Pines, Iterative Carr–Purcell trains, J. Magn. Reson. 77 (1988) 606–611.
[18] T. Gullion, D.B. Baker, M.S. Conradi, New, compensated Carr–Purcell sequences, J. Magn. Reson. 89 (1990) 479–484.
[19] A. Ziegler, M. Decorps, C. Remy, T_2 Measurements with the Carr–Purcell–Meiboom–Gill sequence in the inhomogeneous RF field of surface coils, J. Magn. Reson. 96 (1992) 589–595.
[20] R.L. Vold, R.R. Vold, H.E. Simon, Errors in measurements of transverse relaxation rates, J. Magn. Reson. 11 (1973) 283–298.
[21] T.E. Bull, Effect of RF field inhomogeneities on spin-echo measurements, Rev. Sci. Instrum. 45 (1974) 232–242.
[22] D.G. Hughes, Errors in T_2 values measured with the Carr–Purcell–Meiboom–Gill pulsed NMR sequence, J. Magn. Reson. 26 (1977) 481–489.
[23] D.G. Hughes, G. Lindblom, Baseline drift in the Carr–Purcell–Meiboom–Gill pulsed NMR experiment, J. Magn. Reson. 26 (1977) 469–479.
[24] S. Majumdar, S.C. Orphanoudakis, A. Gmitro, M. O'Donnell, J.C. Gore, Errors in the measurements of T_2 using multiple-echo MRI techniques. I. Effects of radiofrequency pulse imperfections, Magn. Reson. Med. 3 (1986) 397–417.
[25] S. Majumdar, S.C. Orphanoudakis, A. Gmitro, M. O'Donnell, J.C. Gore, Errors in the measurements of T_2 using multiple-echo MRI techniques. II. Effects of static field inhomogeneity, Magn. Reson. Med. 3 (1986) 562–574.
[26] G.J. Barker, T.H. Mareci, Suppression of artifacts in multiple-echo magnetic resonance, J. Magn. Reson. 83 (1989) 11–28.
[27] J. Simbrunner, R. Stollberger, Analysis of Carr–Purcell sequences with nonideal pulses, J. Magn. Reson., Ser. B 109 (1995) 301–309.
[28] M.D. Hürlimann, Carr–Purcell sequences with composite pulses, J. Magn. Reson. 152 (2001) 109–123.
[29] M.D. Hürlimann, Optimization of timing in the Carr–Purcell–Meiboom–Gill sequence, Magn. Reson. Imaging 19 (2001) 375–378.
[30] A. Ross, M. Czisch, G.C. King, Systematic errors associated with the CPMG pulse sequence and their effect on motional analysis of biomolecules, J. Magn. Reson. 124 (1997) 355–365.
[31] M. Czisch, G.C. King, A. Ross, Removal of systematic errors associated with off-resonance oscillations in T_2 measurements, J. Magn. Reson. 126 (1997) 154–157.
[32] D.M. Korzhnev, E.V. Tischenko, A.S. Arseniev, Off-resonance effects in ^{15}N T_2 CPMG measurements, J. Biomol. NMR 17 (2000) 231–237.
[33] N.H. Pawley, M.D. Clark, R. Michalczyk, Rectifying system-specific errors in NMR relaxation measurements, J. Magn. Reson. 178 (2006) 77–87.
[34] P.J. Hajduk, D.A. Horita, L.E. Lerner, Theoretical analysis of relaxation during shaped pulses. I. The effects of short T_1 and T_2, J. Magn. Reson., Ser. A 103 (1993) 40–52.
[35] B.W. Goodwin, R. Wallace, Calculation of response in nuclear magnetic resonance: II. Pulsed experiments, J. Magn. Reson. 9 (1973) 280–290.
[36] J. Jeener, Superoperators in magnetic resonance, Adv. Magn. Reson. 10 (1982) 1–51.
[37] P. Allard, M. Helgstrand, T. Härd, The complete homogeneous master equation for a heteronuclear two-spin system in the basis of Cartesian product operators, J. Magn. Reson. 134 (1998) 7–16.
[38] H.C. Torrey, Transient nutations in nuclear magnetic resonance, Phys. Rev. 76 (1949) 1059–1068.
[39] R.V. Mulkern, M.L. Williams, The general solution to the Bloch equation with constant RF and relaxation terms: application to saturation and slice selection, Med. Phys. 20 (1993) 5–13.
[40] G.A. Morris, P.B. Chilvers, General analytical solutions of the Bloch equations, J. Magn. Reson., Ser. A 107 (1994) 236–238.
[41] G.A. Morris, P.B. Chilvers, Erratum: 107 (2) series A (1994) in the note, General analytical solutions of the Bloch equations, by Gareth A. Morris, Paul B. Chilvers, pp. 236–238, J. Magn. Reson., Ser. A 111 (1994) 232–232.
[42] P.K. Madhu, A. Kumar, Direct Cartesian-space solutions of generalized Bloch equations in the rotating frame, J. Magn. Reson., Ser. A 114 (1995) 201–211.
[43] P.K. Madhu, A. Kumar, Bloch equations revisited: new analytical solutions for the generalized Bloch equations, Concepts Magn. Reson. 9 (1997) 1–12.
[44] D.E. Rourke, A.A. Karabanov, G.H. Booth, I. Frantsuzov, The Bloch equations when $T_1 = T_2$, Inverse Prob. 23 (2007) 609–623.
[45] M. Zweckstetter, T.A. Holak, An adiabatic multiple spin-echo pulse sequence: removal of systematic errors due to pulse imperfections and off-resonance effects, J. Magn. Reson. 133 (1998) 134–147.
[46] G.Q. Zhang, G.J. Hirasaki, CPMG relaxation by diffusion with constant magnetic field gradient in a restricted geometry: numerical simulation and application, J. Magn. Reson. 163 (2003) 81–91.
[47] F. Massi, E. Johnson, C. Wang, M. Rance, A.G. Palmer, NMR $R_{1\rho}$ rotating-frame relaxation with weak radio frequency fields, J. Am. Chem. Soc. 126 (2004) 2247–2256.
[48] A.J. Wheaton, A. Borthakur, M.T. Corbo, G. Moonis, E. Melhem, R. Reddy, $T_{2\rho}$-Weighted contrast in MR images of the human brain, Magn. Reson. Med. 52 (2004) 1223–1227.
[49] N.N. Lukzen, A.A. Savelov, Analytical derivation of multiple spin echo amplitudes with arbitrary refocusing angle, J. Magn. Reson. 185 (2007) 71–76.
[50] D. Hughes-Hallett, A.M. Gleason, W.G. McCallum, B.G. Osgood, D.E. Flath, D. Quinney, P.F. Lock, K. Rhea, D.O. Lomen, J. Tecosky-Feldman, D. Lovelock, T.W. Tucker, Calculus: Single Variable, J. Wiley, Hoboken, NJ, 2009.
[51] G.S. Uhrig, Keeping a quantum bit alive by optimized π-pulse sequences, Phys. Rev. Lett. 98 (2007). 100504-1–4.

[52] J.R. West, B.H. Fong, D.A. Lidar, Near-optimal dynamical decoupling of a Qubit, Phys. Rev. Lett. 104 (2010). 130501-1–4.
[53] P.-O. Löwdin, The normal constants of motion in quantum mechanics treated by projection technique, Rev. Modern Phys. 34 (1962) 520–530.
[54] T.M. Apostol, Some explicit formulas for the exponential matrix e^{tA}, Am. Math. Monthly 76 (1969) 289–292.
[55] E. Freitag, R. Busam, Complex Analysis, Springer, Berlin, Heidelberg, 2005.
[56] R. Fourer, D.M. Gay, B.W. Kernighan, A modeling language for mathematical programming, Manage. Sci. 36 (1990) 519–554.
[57] A. Wächter, L.T. Biegler, On the implementation of an interior-point filter line-search algorithm for large-scale nonlinear programming, Math. Program., Ser. A 106 (2006) 25–57.
[58] S. Mattila, Measurement and Minimization of Field Inhomogeneities in High Resolution NMR, University of Oulu, 2001.